Exact calculation of the magnetocaloric effect in the spin-$\frac{1}{2}$ *XXZ* chain

Christian Trippe,[1] Andreas Honecker,[2] Andreas Klümper,[1] and Vadim Ohanyan[3,4]
[1]*Theoretische Physik, Universität Wuppertal, Gauß-Str. 20, 42097 Wuppertal, Germany*
[2]*Institut für Theoretische Physik, Georg-August-Universität Göttingen, 37077 Göttingen, Germany*
[3]*Department of Theoretical Physics, Yerevan State University, Al. Manoogian 1, 0025 Yerevan, Armenia*
[4]*Yerevan Physics Institute, Alikhanian Brothers 2, 0036 Yerevan, Armenia*
(Received 18 September 2009; revised manuscript received 24 December 2009; published 2 February 2010)

We calculate the entropy and cooling rate of the antiferromagnetic spin-$\frac{1}{2}$ *XXZ* chain under an adiabatic demagnetization process using the quantum transfer-matrix technique and nonlinear integral equations. The limiting case of the Ising chain (corresponding to infinitely large anisotropy) is presented for comparison. Our exact results for the Heisenberg chain are used as a cross-check for the numerical exact diagonalization as well as quantum Monte Carlo simulations and allow us to benchmark the numerical methods. Close to field-induced quantum phase transitions we observe a large magnetocaloric effect. Furthermore, we verify universal low-temperature power laws in the cooling rate and entropy, in particular, linear scaling of entropy with temperature T in the gapless Luttinger-liquid state and scaling as $\sqrt{T}$ at field-induced transitions to gapped phases.

DOI: 10.1103/PhysRevB.81.054402 PACS number(s): 75.10.Pq, 75.30.Sg, 02.70.−c

I. INTRODUCTION

The magnetocaloric effect (MCE), in general, addresses the change in temperature of magnetic systems under the variation of an external magnetic field. The MCE has been known since the end of the 19th century[1] and it has attracted renewed interest recently because of potential room-temperature cooling applications (see Refs. 2 and 3 for recent reviews). On the other hand, adiabatic demagnetization is a standard low-temperature method: demagnetization of paramagnetic salts was the first method to reach temperatures below 1 K (Ref. 4) whereas demagnetization of nuclear spins has reached record low temperatures down to 100 pK (Refs. 5 and 6) and is still the cooling method of choice in the microkelvin range.[7] The cooling rate at the adiabatic demagnetization $(\frac{\partial T}{\partial H})_S$ for an ideal paramagnet (i.e., a system of noninteracting magnetic moments) is equal to T/H, which means linear monotonic dependence of temperature on the magnetic field magnitude. The latter is a direct consequence of the fact that for any paramagnetic system the entropy depends only on the ratio H/T, so for any isentrope one gets H/T=const. However, the matter could undergo crucial changes for systems of interacting spins. For instance, in ferromagnets near the Curie point one can observe a substantial enhancement of the effect.[8]

As has been shown in early investigations, quantum antiferromagnets are more efficient low-temperature magnetic coolers than ferromagnets.[9–11] This fact is connected with the behavior of the entropy of antiferromagnets. The entropy of any antiferromagnet at low temperatures displays (at least) one maximum as a function of magnetic field, which usually, according to the third law of thermodynamics, falls to zero at $T\to 0$.[10] The Ising model is anomalous, in this respect, because of nonvanishing zero-temperature entropy at the critical magnetic field $H_c=qJ$, where q is the coordination number of the lattice and J is the coupling constant. Indeed, understanding the influence of quantum fluctuations seems to have been an important motivation for the numerical work Ref. 10. The first exact result concerning magnetocaloric properties of the spin-$\frac{1}{2}$, Ising-type *XXZ* chain has been obtained in Ref. 11, where the isentropes in the (H,T) plane have been presented. The main feature of the isentropes of the Ising-type *XXZ* chain is the appearance of two minima. To the best of our knowledge, the isentropes of the isotropic-spin-$\frac{1}{2}$ Heisenberg chain have so far been investigated only numerically[12] (for numerical studies of the magnetocaloric effect in ferrimagnetic spin chains and higher-spin Heisenberg chains see Refs. 13 and 14). Recent measurements[15] of the adiabatic cooling rate in the spin-$\frac{1}{2}$ Heisenberg chain compound $[\mathrm{Cu}(\mu\text{-}\mathrm{C_2O_4})(4\text{-aminopyridine})_2(\mathrm{H_2O})]_n$ render the magnetocaloric effect of the spin-$\frac{1}{2}$ Heisenberg chain a topic of current interest.

More generally, the MCE is particularly large in the vicinity of quantum critical points (QCPs). The MCE is closely related to the generalized Grüneisen ratios

$$\Gamma_r = -\frac{1}{T}\frac{(\partial S/\partial r)_T}{(\partial S/\partial T)_r}. \tag{1}$$

Here r is the control parameter governing the quantum phase transition. In the case of the MCE r is the external magnetic field H. Using basic thermodynamic relations,[3] the generalized Grüneisen ratio Γ_H can be related to the adiabatic cooling rate $(\partial T/\partial H)_S$,[16,17]

$$\Gamma_H = \frac{1}{T}\left(\frac{\partial T}{\partial H}\right)_S = -\frac{1}{C_H}\left(\frac{\partial M}{\partial T}\right)_H. \tag{2}$$

Thus, the magnetic cooling rate is an important quantity for the characterization of QCPs, i.e., quantum phase transitions between different magnetic structures under tuning the magnetic field at $T=0$.

In passing we mention that an analysis of classical spin models[18] demonstrated that the MCE can be enhanced by geometric frustration. Indeed, adiabatic demagnetization experiments on the frustrated spin-$\frac{7}{2}$ pyrochlore-type magnet $\mathrm{Gd_2Ti_2O_7}$ have shown substantial drops in temperature in the

vicinity of the saturation field.[19] Enhanced cooling performance is also theoretically predicted in one-dimensional quantum antiferromagnets such as the J_1-J_2 chain and the sawtooth chain,[12] the diamond chain,[20–24] as well as in two dimensions.[25,26]

The one-dimensional spin-$\frac{1}{2}$ Heisenberg model is famous for its integrability. The conventional Bethe ansatz technique allows one to obtain all eigenvalues and eigenvectors of the corresponding Hamiltonian, though in nonexplicit form. There are several sophisticated methods to describe thermodynamics of one-dimensional integrable models, such as thermodynamic Bethe ansatz (TBA), etc. (see, for example, Refs. 27 and 28). For pragmatical reasons, the most suitable technique is the quantum transfer-matrix (QTM) method leading to only two nonlinear integral equations (NLIE) for the free energy of the Heisenberg chain, see Refs. 29–31 and references therein. A numerical solution of these NLIEs has been used in Ref. 29 to obtain the magnetic susceptibility and specific heat of the isotropic-spin-$\frac{1}{2}$ Heisenberg chain in an external magnetic field. However, as far as we are aware, there are no exact results for the free energy (or equivalently the entropy) and a mixed derivative of the free energy which corresponds to the magnetic cooling rate in the literature for the isotropic spin-$\frac{1}{2}$ Heisenberg chain. Filling these gaps is one of the purposes of the present paper.

In this paper we present calculations of quantities related to the MCE for the one-dimensional spin-$\frac{1}{2}$ *XXZ* Heisenberg chain within the QTM and NLIE methods. Particularly, isentropes for different values of the exchange anisotropy parameter Δ are obtained. The cooling rate is computed as a function of external magnetic field for various fixed values of temperature and different values of the exchange anisotropy. The limiting case of infinitely large anisotropy which is just the Ising model is considered as well. In that case the expressions for all relevant thermodynamic quantities can be obtained in closed form. These calculations are supplemented by exact diagonalization (ED) and quantum Monte Carlo (QMC) calculations demonstrating full agreement between results obtained from the exact solution and numerical calculations.

II. ISENTROPES AND COOLING RATE FOR THE SPIN-$\frac{1}{2}$ *XXZ* HEISENBERG CHAIN

We will be interested both in the entropy and the associated isentropes as well as the temperature derivatives thereof, i.e., the adiabatic cooling rate $(\frac{\partial T}{\partial H})_S$. Using standard thermodynamic relations one can express the latter as follows:[3]

$$\left(\frac{\partial T}{\partial H}\right)_S = -\frac{T}{C_H}\left(\frac{\partial M}{\partial T}\right)_H, \tag{3}$$

where C_H is the specific heat at constant magnetic field and M is the magnetization of the system. After normalization with a factor $1/T$, the magnetic cooling rate can be identified with the generalized Grüneisen ratio Eq. (2) which we will use in the following.

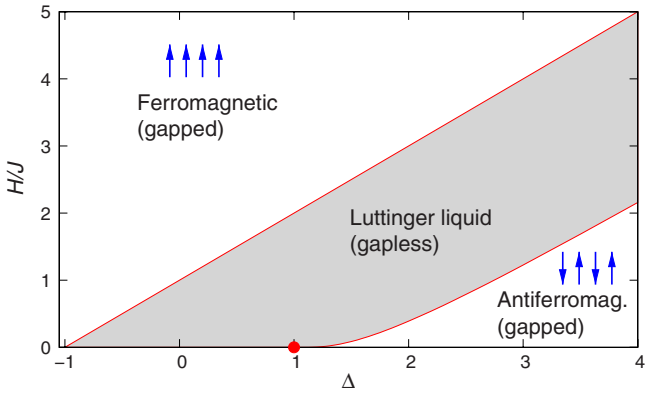

FIG. 1. (Color online) Zero-temperature phase diagram of the spin-$\frac{1}{2}$ *XXZ* chain in a magnetic field.

We will be specifically interested in the spin-$\frac{1}{2}$ *XXZ* Heisenberg chain whose Hamiltonian is given by

$$\mathcal{H} = J\sum_{n=1}^{N}\left(S_n^x S_{n+1}^x + S_n^y S_{n+1}^y + \Delta S_n^z S_{n+1}^z\right) - H\sum_{n=1}^{N} S_n^z. \tag{4}$$

Here N is the total number of sites, S_n^α are spin-$\frac{1}{2}$ operators acting at site n, J is the exchange constant, Δ is an exchange asymmetry, and H is an external magnetic field. For the finite-size computations we will assume periodic boundary conditions, i.e., $S_{N+1}^\alpha = S_1^\alpha$. Note that the properties of the *XXZ* model (4) are symmetric under $H \to -H$ and $M = \langle S_n^z \rangle \to -M$. We will therefore concentrate on $H \geq 0$ in the following.

It is useful to recall the zero-temperature phase diagram of the model (4), see Fig. 1.[32–34] For $\Delta > 1$ and small magnetic fields $H < H_{c1}$ there is long-range antiferromagnetic order along the z direction in spin space. This state exhibits a gap in the excitation spectrum whose value at $H=0$ corresponds to H_{c1}. The value of the gap has been computed exactly via the Bethe ansatz.[35,36] In particular, it is exponentially small close to the Heisenberg point at $\Delta = 1$ (marked by the dot in Fig. 1), which is characteristic for a Kosterlitz-Thouless transition.[37,38] For $\Delta < 1$, one finds a gapless Luttinger-liquid state.[39] This Luttinger-liquid state exists for $|\Delta| < 1$, $H < H_{c2}$ and $\Delta > 1$, $H_{c1} < H < H_{c2}$, with $H_{c2} = J(1+\Delta)$. Finally, for $H > H_{c2}$, the ground state is the ferromagnetically polarized state along the z direction which exhibits again a gap. We anticipate that these different zero-temperature regions, in particular, the quantum phase transitions at H_{c1} and H_{c2} will be reflected by the magnetocaloric properties at finite temperature.

A. Nonlinear integral equations

In this section we recall the approach to the thermodynamics using the QTM technique and NLIEs.[29,31] The equations look different for $|\Delta| < 1$ and $|\Delta| > 1$.

First we consider the case $|\Delta| < 1$. One can represent the free energy of the system per lattice site in the following form:

$$f = e_0 - T\int_{-\infty}^{\infty} \frac{\ln\{[1+a(x)][1+\bar{a}(x)]\}}{4\cosh\frac{\pi x}{2}}dx \tag{5}$$

(the constant e_0 is irrelevant in the present context). The auxiliary functions $a(x)$ and $\bar{a}(x)$ are found from the following system of integral equations:

$$\ln a(x) = -\frac{J\sin\gamma}{T2\gamma}\frac{\pi}{\cosh\frac{\pi x}{2}} + \frac{\pi H}{2T(\pi-\gamma)} + \kappa * \ln(1+a)(x) - \kappa^{+} * \ln(1+\bar{a})(x), \tag{6a}$$

$$\ln \bar{a}(x) = -\frac{J\sin\gamma}{T2\gamma}\frac{\pi}{\cosh\frac{\pi x}{2}} - \frac{\pi H}{2T(\pi-\gamma)} + \kappa * \ln(1+\bar{a})(x) - \kappa^{-} * \ln(1+a)(x). \tag{6b}$$

Here $\gamma=\arccos\Delta$, the symbol $*$ denotes convolution $f*g(x)=\int_{-\infty}^{\infty}f(x-y)g(y)dy$ and the function $\kappa(x)$ is defined by

$$\kappa(x) = \frac{1}{2\pi}\int_{-\infty}^{\infty}\frac{\sinh\left(\frac{\pi}{\gamma}-2\right)k}{2\cosh k\sinh\left(\frac{\pi}{\gamma}-1\right)k}e^{ikx}dk,$$

$$\kappa^{\pm}(x) = \kappa(x \pm 2i). \tag{7}$$

These equations are valid for $0<\Delta<1$. Results for negative Δ can be obtained by changing the sign of the coupling J.

For the case $\Delta>1$ the free energy has the form

$$f = e_0 - \frac{T}{2}c \star \ln[(1+\mathfrak{b})(1+\bar{\mathfrak{b}})](0) = e_0 - \frac{T}{2\pi}\int_{-\pi/2}^{\pi/2} c(x)\ln\{[1+\mathfrak{b}(x)][1+\bar{\mathfrak{b}}(x)]\}dx \tag{8}$$

with $f\star g(x)=\frac{1}{\pi}\int_{-\pi/2}^{\pi/2}dy f(x-y)g(y)$ denoting a convolution with modified integration limits and

$$c(x) = \sum_{k=-\infty}^{\infty}\frac{1}{\cosh(\eta k)}e^{i2kx} \tag{9}$$

with $\Delta=\cosh\eta$. The auxiliary functions are solutions of the following integral equations:

$$\ln\mathfrak{b}(x) = -\frac{J\sinh(\eta)}{2T}c(x) + \frac{H}{2T} + k\star\ln[1+\mathfrak{b}(x)] - k^{+}\star\ln[1+\bar{\mathfrak{b}}(x)] \tag{10a}$$

$$\ln\bar{\mathfrak{b}}(x) = -\frac{J\sinh(\eta)}{2T}c(x) - \frac{H}{2T} + k\star\ln[1+\bar{\mathfrak{b}}(x)] - k^{-}\star\ln[1+\mathfrak{b}(x)] \tag{10b}$$

with integration kernels

$$k(x) = \sum_{k=-\infty}^{\infty}\frac{e^{-\eta|k|}}{2\cosh(\eta k)}e^{i2kx}, \quad k^{\pm}(x) = k(x\pm i\eta^{\mp}). \tag{11}$$

Results for $\Delta<-1$ can again be obtained by changing the sign of the coupling J.

The equations for the isotropic case $\Delta=1$ can be obtained by taking the limit $\gamma\to 0$ from the case $|\Delta|<1$ in Eqs. (5) and (6) or from the case $|\Delta|>1$ by changing the spectral parameter $x=\tilde{x}\eta$ and taking the limit $\eta\to 0$ in Eqs. (8) and (10).

Having all these exact expressions one can obtain any thermodynamic quantity of interest by iteration of the NLIE in Eq. (6) [or Eq. (10)] and numerical integration of the expression for the free energy in Eq. (5) [or Eq. (8)]. Derivatives of the free energy with respect to T and H can also be calculated. One can avoid numerical differentiation by solving the associated integral equations for the differentiated auxiliary functions, e.g., $\partial_H \ln a(x)$. Note that derivatives of $\ln a(x)$ and $\ln\bar{a}(x)$ are treated as independent functions in these equations. As an example we will give the equations for the calculation of the magnetization per spin M and the derivative of M with respect to the temperature in the regime $|\Delta|<1$

$$M = T\int_{-\infty}^{\infty}\frac{1}{4\cosh\frac{\pi x}{2}}\left\{\frac{a(x)}{1+a(x)}[\partial_H\ln a(x)] + \frac{\bar{a}(x)}{1+\bar{a}(x)}[\partial_H\ln\bar{a}(x)]\right\}dx. \tag{12}$$

The derivatives $\partial_H\ln a(x)$ and $\partial_H\ln\bar{a}(x)$ satisfy *linear* integral equations in which the auxiliary functions $a(x)$ and $\bar{a}(x)$ enter as external functions

$$\partial_H\ln a(x) = \frac{\pi}{2T(\pi-\gamma)} + \kappa * \frac{a}{1+a}[\partial_H\ln a](x) - \kappa * \frac{\bar{a}}{1+\bar{a}}[\partial_H\ln\bar{a}](x+2i), \tag{13a}$$

$$\partial_H\ln\bar{a}(x) = -\frac{\pi}{2T(\pi-\gamma)} + \kappa * \frac{\bar{a}}{1+\bar{a}}[\partial_H\ln\bar{a}](x) - \kappa * \frac{a}{1+a}[\partial_H\ln a](x-2i). \tag{13b}$$

To obtain the cooling rate Γ_H we have to determine $\partial M/\partial T$. In order to achieve this we have to differentiate [Eq. (12)] with respect to T. However it has turned out that in the framework of NLIEs the resulting equations, in general, behave numerically better if the derivatives are taken with respect to the inverse temperature $\beta=1/T$ (we set $k_B=1$),

$$\left(\frac{\partial M}{\partial T}\right)_H = -\beta^2\left(\frac{\partial M}{\partial \beta}\right)_H$$
$$= \int_{-\infty}^{\infty} \frac{1}{4\cosh\frac{\pi x}{2}}\left\{\frac{a(x)}{1+a(x)}[\partial_H \ln a(x)] + \frac{\bar{a}(x)}{1+\bar{a}(x)}[\partial_H \ln \bar{a}(x)]\right\}dx$$
$$- \beta\int_{-\infty}^{\infty} \frac{1}{4\cosh\frac{\pi x}{2}}\left(\left\{\frac{a(x)}{1+a(x)} - \left[\frac{a(x)}{1+a(x)}\right]^2\right\}\right.$$
$$\times[\partial_\beta \ln a(x)][\partial_H \ln a(x)] + \frac{a(x)}{1+a(x)}[\partial_\beta\partial_H \ln a(x)]$$
$$+ \left\{\frac{\bar{a}(x)}{1+\bar{a}(x)} - \left[\frac{\bar{a}(x)}{1+\bar{a}(x)}\right]^2\right\}[\partial_\beta \ln \bar{a}(x)]$$
$$\left.\times[\partial_H \ln \bar{a}(x)] + \frac{\bar{a}(x)}{1+\bar{a}(x)}[\partial_\beta\partial_H \ln \bar{a}(x)]\right)dx. \quad (14)$$

Here four new functions $\partial_\beta \ln a(x)$, $\partial_\beta\partial_H \ln a(x)$, and their $\bar{a}$ counterparts occur. The corresponding linear integral equations read

$$\partial_\beta \ln a(x) = -\frac{J\sin\gamma}{2\gamma}\frac{\pi}{\cosh\frac{\pi x}{2}} + \frac{\pi H}{2(\pi-\gamma)} + \kappa * \frac{a}{1+a}[\partial_\beta \ln a](x) - \kappa^+ * \frac{\bar{a}}{1+\bar{a}}[\partial_\beta \ln \bar{a}](x), \quad (15a)$$

$$\partial_\beta \ln \bar{a}(x) = -\frac{J\sin\gamma}{2\gamma}\frac{\pi}{\cosh\frac{\pi x}{2}} - \frac{\pi H}{2(\pi-\gamma)} + \kappa * \frac{\bar{a}}{1+\bar{a}}[\partial_\beta \ln \bar{a}](x) - \kappa^- * \frac{a}{1+a}[\partial_\beta \ln a](x) \quad (15b)$$

and

$$\partial_\beta\partial_H \ln a(x) = \frac{\pi}{2(\pi-\gamma)} + \kappa * \left\{\left[\frac{a}{1+a} - \left(\frac{a}{1+a}\right)^2\right][\partial_\beta \ln a]\right.$$
$$\times[\partial_H \ln a] + \frac{a}{1+a}[\partial_\beta\partial_H \ln a]\Big\}(x)$$
$$- \kappa^+ * \left\{\left[\frac{\bar{a}}{1+\bar{a}} - \left(\frac{\bar{a}}{1+\bar{a}}\right)^2\right][\partial_\beta \ln \bar{a}][\partial_H \ln \bar{a}]\right.$$
$$\left.+ \frac{\bar{a}}{1+\bar{a}}[\partial_\beta\partial_H \ln \bar{a}]\right\}(x), \quad (16a)$$

$$\partial_\beta\partial_H \ln \bar{a}(x) = -\frac{\pi}{2(\pi-\gamma)} + \kappa * \left\{\left[\frac{\bar{a}}{1+\bar{a}} - \left(\frac{\bar{a}}{1+\bar{a}}\right)^2\right]\right.$$
$$\times[\partial_\beta \ln \bar{a}][\partial_H \ln \bar{a}] + \frac{\bar{a}}{1+\bar{a}}[\partial_\beta\partial_H \ln \bar{a}]\Big\}(x)$$
$$- \kappa^- * \left\{\left[\frac{a}{1+a} - \left(\frac{a}{1+a}\right)^2\right][\partial_\beta \ln a][\partial_H \ln a]\right.$$
$$\left.+ \frac{a}{1+a}[\partial_\beta\partial_H \ln a]\right\}(x). \quad (16b)$$

Note that the functions $\partial_\beta \ln a(x)$ and $\partial_\beta \ln \bar{a}(x)$ already allow the calculation of the entropy per spin

$$S = \int_{-\infty}^{\infty} \frac{\ln\{[1+a(x)][1+\bar{a}(x)]\}}{4\cosh\frac{\pi x}{2}}dx - \frac{1}{T}\int_{-\infty}^{\infty} \frac{1}{4\cosh\frac{\pi x}{2}}\left\{\frac{a(x)}{1+a(x)}[\partial_\beta \ln a(x)] + \frac{\bar{a}(x)}{1+\bar{a}(x)}[\partial_\beta \ln \bar{a}(x)]\right\}dx. \quad (17)$$

For the calculation of the cooling rate Γ_H the specific heat is needed in addition to the mixed derivative $\partial M/\partial T$. It can be obtained by differentiating Eq. (17) with respect to β and dividing by $-T$. In the resulting equation another pair of functions $\partial_\beta^2 \ln a(x)$ and $\partial_\beta^2 \ln \bar{a}(x)$ occurs, where the corresponding integral equations are derived by differentiating Eq. (15) again with respect to β in close analogy to Eq. (16).

B. Comparison with numerical results

First, we present a comparison with numerical methods, namely, ED and QMC. On the one hand, this comparison will serve as a cross-check of our results. On the other hand, we can use the exact results to assess the performance of the numerical methods.

The quantities appearing on the right-hand side of Eq. (2) can be expressed as follows:

$$C_H = \frac{\beta^2}{N}(\langle\mathcal{H}^2\rangle - \langle\mathcal{H}\rangle^2), \quad (18)$$

$$\left(\frac{\partial M}{\partial T}\right)_H = \frac{\beta^2}{N}(\langle M\mathcal{H}\rangle - \langle M\rangle\langle\mathcal{H}\rangle), \quad (19)$$

where $\langle\cdot\rangle$ is the expectation value at a fixed temperature T and magnetic field H. Here we have chosen a normalization per spin which drops out when taking the ratio in Eq. (2). Equation (18) is well known and Eq. (19) is valid for any Hamiltonian conserving magnetization, i.e., $[M,\mathcal{H}]=0$.

One can write down spectral representations for the correlation functions in Eqs. (18) and (19) which can be evaluated by ED. These correlation functions can also be evaluated with QMC. The QMC simulations to be reported below have been carried out with the ALPS (Algorithms and

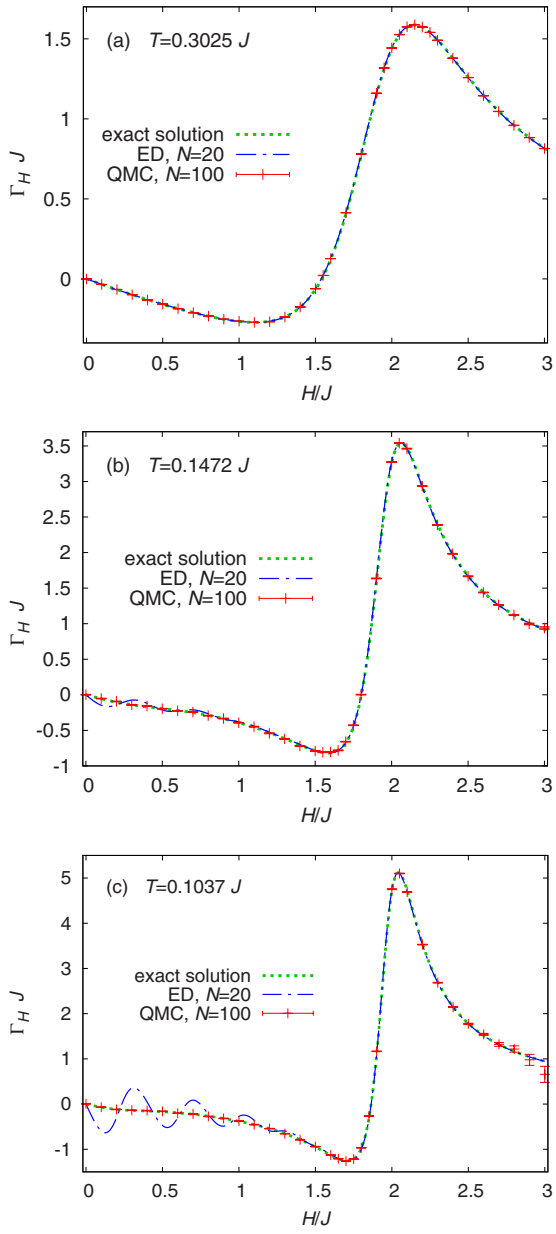

FIG. 2. (Color online) Cooling rate Γ_H for the Heisenberg chain ($\Delta=1$). Shown are ED for $N=20$ sites, QMC for $N=100$ sites, and the exact solution for the infinite system. The different panels are for (a) $T/J=0.3025$, (b) 0.1472, and (c) 0.1037.

Libraries for Physics Simulations, Refs. 40 and 41) directed loop application[42] in the stochastic series-expansion framework.[43] The specific heat, Eq. (18), is measured using an improved estimator which involves the fluctuations of the expansion order.[44] The correlation function, Eq. (19), can be measured in a similar manner. Note that it is crucial to choose an appropriate pseudorandom-number generator in order to obtain correct results. We have used the "Mersenne Twister."[45] In our QMC simulations we have performed 4×10^5 thermalization steps and then collected data during a number of sweeps ranging between 2×10^7 and 3.3×10^{10}.

Figure 2 shows a comparison of Γ_H between the exact solution for $N=\infty$, ED for $N=20$, and QMC for $N=100$ at three temperatures which have been chosen to correspond to the experiments of Ref. 15. The ED curves exhibit some wiggles at small magnetic fields and temperatures which reflect the fact that the system contains only $N=20$ sites. In this regime, the QMC results for $N=100$ are indistinguishable from the exact solution for $N=\infty$ on the scale of Fig. 2. On the other hand, the QMC results are subject to big error bars at *high* fields and low temperatures despite the fact that we have invested substantial amounts of CPU time into these data points. To some extent, this is related to performance problems of the algorithm in a magnetic field.[43] However, the main reason is that Γ_H is given by the ratio of two quantities [see Eq. (2)] which are both exponentially small in T for $H>H_{c2}=2J$. Indeed, even with a large number of sweeps, it is difficult to determine the ratio of two very small quantities accurately by QMC. Conversely, the existence of a gap improves finite-size convergence such that ED works particularly well in the high-field regime.

The overall good agreement between all three methods serves as a consistency check for each of them. Furthermore, we see that we can get extremely accurate numerical results by combining QMC for $H\lesssim H_{c2}$ and ED for $H\gtrsim H_{c2}$ ($H_{c2}=2J$ in the present case).

C. Effects of anisotropy Δ

Next, we discuss the effects of exchange anisotropy on the cooling rate. Figure 3 shows results for three selected values $\Delta=0.5$, 1, and 2. Recall from Fig. 1 that, at $\Delta=0.5$, one crosses just one quantum phase transition at $H_{c2}=1.5J$, the curves for $\Delta=1$ in Fig. 3 start from the special Heisenberg point at $H=0$ and cross the transition to saturation at $H_{c2}=2J$, and the curves at $\Delta=2$ cut two quantum phase transitions, namely, $H_{c1}\approx0.39J$ and $H_{c2}=3J$. For $T=0.05J$, the quantum phase transitions at H_{c2} and for $\Delta=2$ at H_{c1} are signaled by sign changes in the cooling rate Γ_H from negative to positive values upon increasing field, see Fig. 3(a). Note that these zeros shift away from the position of the zero-temperature phase transitions with increasing temperature, as is evident, in particular, if one takes into account the additional data for $\Delta=1$ shown in Fig. 2. Finally, there is a small structure at low magnetic fields in the $\Delta=1$ curves of Figs. 2(c) and 3(a) which reflects the singular nature of the Heisenberg point ($\Delta=1, H=0$).

At the isotropic point of the antiferromagnetic *XXZ* chain, the quantity Γ_H/H shows singular behavior for $T\to0$ if $H<T$. In fact, in the limit of $H\to0$ the ratio reduces to the temperature derivative of the zero-field susceptibility $\chi(T)$

$$\lim_{H\to0}\frac{\Gamma_H(T)}{H}=-\frac{1}{C_H}\left(\frac{\partial\chi}{\partial T}\right)_H, \tag{20}$$

which is known to show singular behavior. For $\Delta=1$ this function diverges like const$\times[T\ln(T_0/T)]^{-2}$ where T_0 is a (nonuniversal) constant.[46] For $\Delta<1$ the function in Eq. (20) diverges like const$\times T^{4K-6}$ with Tomonaga-Luttinger parameter $K=\pi/(\pi-\gamma)>1$.[47] For $\Delta>1$ a divergent behavior like const$/T$ is observed. The strongest divergence is hence exhibited for $\Delta=1$. For finite magnetic field H we see a nondivergent behavior for $T\to0$.

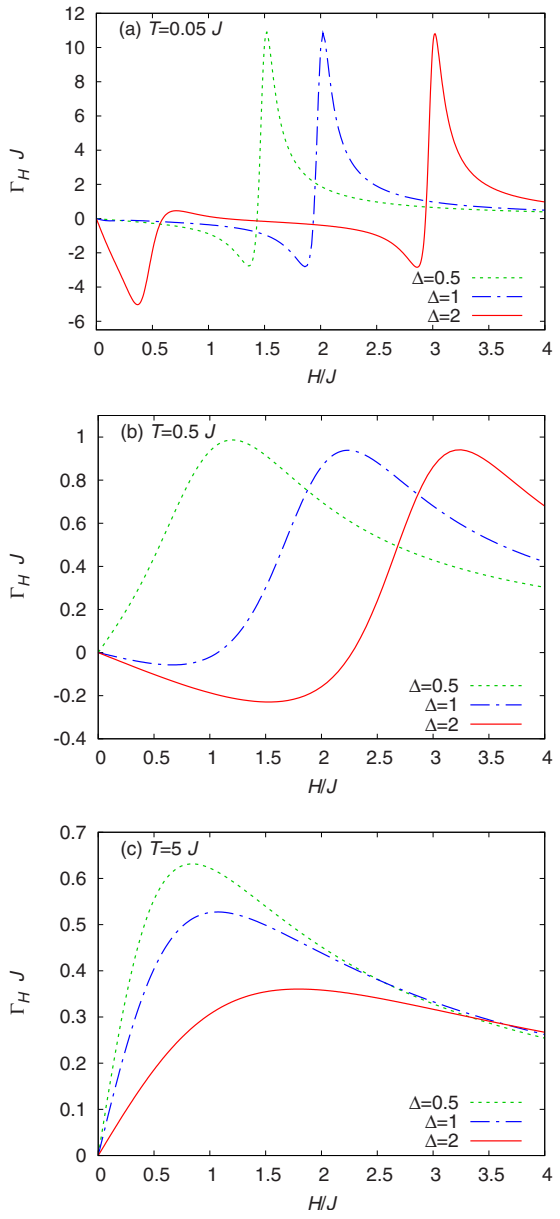

FIG. 3. (Color online) Cooling rate Γ_H for different values of the anisotropy. Shown is the exact solution for the infinite system. The different panels are for (a) $T/J=0.05$, (b) 0.5, and (c) 5.

With increasing temperature, all features become broader. Note that the temperature $T=0.5J$ shown in Fig. 3(b) is higher than the value of H_{c1} at $\Delta=2$ which explains why the sign change around H_{c1} in the $\Delta=2$ curve disappears for $T=0.5J$. For the even higher temperature $T=5J$ shown in Fig. 3(c), the cooling rate Γ_H is positive for all $H>0$ (the zero at $H=0$ is enforced by the symmetry under $H\rightarrow -H$). Note that $T=5J$ is bigger than H_{c2} itself for all cases shown in Fig. 3(c) which explains why all features are washed out at this temperature.

D. Case of infinitely large anisotropy: Cooling rate for the Ising chain

The case of infinitely large anisotropy ($\Delta\rightarrow\infty$ at $J_I=J\Delta=$const) corresponds to the Ising model with Hamiltonian

$$\mathcal{H}=J\sum_{i=1}^{N}s_is_{i+1}-H\sum_{i=1}^{N}s_i, \tag{21}$$

where the classical variables s_i take values $\pm 1/2$ and for simplicity reasons we drop the subscript of the coupling J_I in this section. It is well known that the Ising chain can be solved exactly and completely analytically by the transfer-matrix method (see, for example, Refs. 48 and 49) and even $(\partial M/\partial T)_H$ was investigated recently.[50] However, we are not aware of explicit results for the entropy S and normalized cooling rate Γ_H of the Ising chain and therefore present them here.

We start from the free energy per lattice site of the Ising chain,

$$f=-\frac{1}{\beta}\ln\{e^{-\beta J/4}[\cosh(\beta H/2)+\sqrt{\sinh^2(\beta H/2)+e^{\beta J}}]\}. \tag{22}$$

From this expression one can easily obtain simple analytic expressions for all thermodynamic functions of the system. In particular, one obtains for the entropy per spin and the normalized cooling rate,

$$S=-\left(\frac{\partial f}{\partial T}\right)_H=\ln[e^{-\beta J/4}(c+Q)] - \frac{-J/4(c+Q)+sH/2+\dfrac{sH/2+Je^{\beta J}}{Q}}{T(c+Q)}, \tag{23}$$

$$\Gamma_H=\frac{1}{T}\left(\frac{\partial T}{\partial H}\right)_S=-\frac{\dfrac{\partial^2 f}{\partial T\,\partial H}}{T\dfrac{\partial^2 f}{\partial T^2}} =\frac{1/2(cH/2-sJ/2)(c+Q)^2}{1/2J^2s^2Q+1/4J^2c(s^2+Q^2)+H/2(cH/2-Js)(c+Q)^2}, \tag{24}$$

where

$$c=\cosh(\beta H/2),\quad s=\sinh(\beta H/2),$$

$$Q=\sqrt{\sinh^2(\beta H/2)+e^{\beta J}}. \tag{25}$$

The $T=0$ limit of the entropy in Eq. (23) is generically $S=0$, except for $H=\pm J$, where one finds $S=\ln(\frac{1+\sqrt{5}}{2})=0.4812\cdots$ (see also Ref. 51). This reflects the macroscopic ground-state degeneracy of the Ising model at the saturation field $H_c=J$.[10] Remarkably, the above transfer-matrix solution is closely related to the hard-dimer description of certain highly frustrated one-dimensional quantum antiferromagnets.[12,22,52–54]

Figure 4 shows the cooling rate dependence on the magnetic field for the Ising chain obtained from the exact solution. The main difference from the *XXZ* case are the very sharp and pronounced positive and negative peaks at the critical value of the magnetic field. The magnitude of these

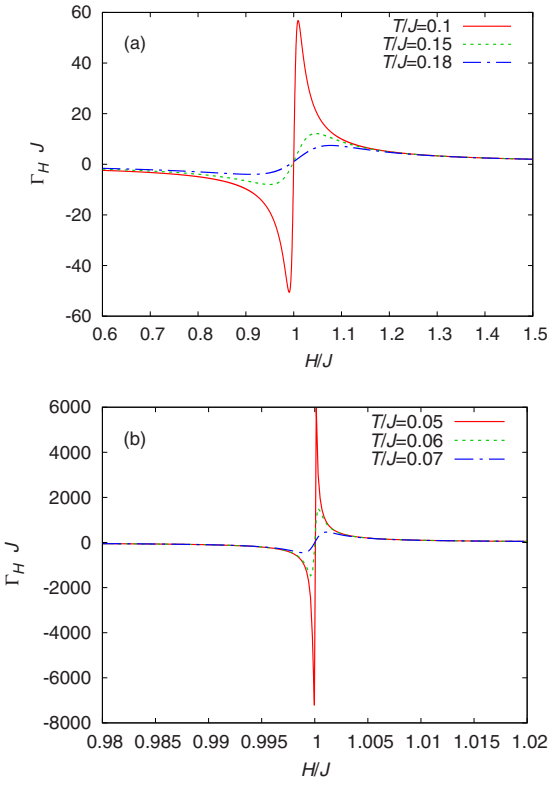

FIG. 4. (Color online) Cooling rate Γ_H of the Ising model ($\Delta \to \infty$ limit of the *XXZ* model). Shown is the exact solution for the infinite system. The different panels show (a) the cooling rate for a wider range of temperatures and (b) the behavior at low temperatures in the vicinity of the critical point.

peaks grows rapidly with decreasing temperature. This behavior is a direct consequence of the anomalous zero-temperature entropy of the Ising chain at $H=J$.[10]

A bit further away from the QCP at $H_c=J$, we can make contact with the argumentation of Ref. 17. The Grüneisen ratio, which in our case is the cooling rate Γ_H, shows divergent behavior close to the QCP at H_c and changes sign when the magnetic field crosses it. For $H \neq H_c$, the divergent behavior obeys the universal scaling law[16,17]

$$\Gamma_H(T \to 0, H) = -G_H \frac{1}{H - H_c}, \tag{26}$$

where G_H is a universal amplitude. Detailed analysis of the Ising case yields the exact analytic form of the cooling rate at extremely low temperatures, $\Gamma_H^{\mathrm{Ising}}(T \to 0) = \frac{1}{H-J}$ for $T \ll |H-J|$, i.e., the value $G_H=-1$ expected for a $\mathbb{Z}_2$ symmetry in one dimension.[12,17]

E. Entropy

Finally, we take a look at the entropy S. As far as we are aware, there has been only one previous attempt of an exact computation[11] of the entropy and accordingly the isentropes of the *XXZ* chain in a magnetic field. Inspection of the critical fields H_{c1} and H_{c2} indicates that the result of Ref. 11 corresponds to an anisotropy $\Delta \approx 4.75$. The main technical difference between Ref. 11 and the present work is that Ref. 11 worked with an infinite hierarchy of equations for $\Delta > 1$ which need to be truncated while we have a closed finite set of equations for all values of Δ. In the case $|\Delta| < 1$ the structure of the NLIE [Eq. (6)] is independent of Δ in contrast to the usual TBA equations, which allows to easily calculate the entropy as a function of the anisotropy.

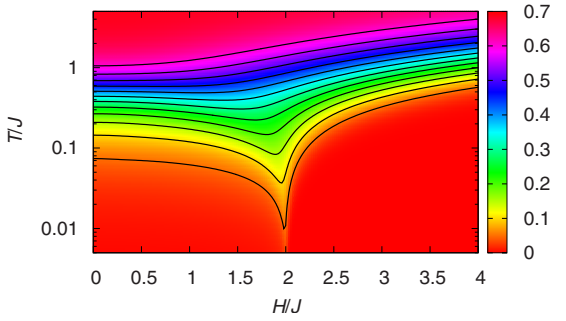

FIG. 5. (Color online) Entropy per spin $S(H,T)$ for $\Delta=1$. The isentropes are for $S=0.05, 0.1, \ldots, 0.6$.

Figure 5 shows the entropy and the isentropes for the spin-$\frac{1}{2}$ Heisenberg chain in the H-T plane. This result agrees with previous ED for $N=20$ sites.[12] However, the ED results of Ref. 12 suffered from finite-size effects, in particular, for low temperatures and $H < H_{c2} = 2J$. By contrast, Fig. 5 shows results for the thermodynamic limit. Figure 6 shows a similar plot of the entropy and isentropes with varying anisotropy Δ but now at a fixed magnetic field H. The quantum phase transitions at H_{c1} and H_{c2} are reflected in Figs. 5 and 6 by minima of the isentropes as a function of H or Δ, or equivalently maxima of the entropy at a low but constant temperature. The only exception is Fig. 6(a) where one observes no such clear signature of the Kosterlitz-Thouless transition at $\Delta=1$ for $H=0$. Before we discuss this case in more detail, it is useful to examine the low-temperature asymptotics of the entropy $S(T)$ at otherwise fixed parameters H and Δ.

Between the two quantum critical points, that is for $H_{c1} < H < H_{c2}$, the low-energy theory is a Luttinger liquid (compare remarks at the beginning of Sec. II). It is well known that the specific heat C of a Luttinger liquid is linear in T.[55] Due to the relation $C = T(\partial S/\partial T)$ (see, e.g., Ref. 3) and because of $S(T=0)=0$, the entropy of a Luttinger liquid is identical to its specific heat and, in particular, also linear

$$S = \frac{\pi}{3v} T \quad \text{for} \quad H_{c1} < H < H_{c2}, \tag{27}$$

where v is the velocity of the excitations.

The cases $H=H_{c1}$ and H_{c2} are instances of a quantum phase transition in one dimension which preserves a U(1) symmetry. In this case, the universal low-temperature asymptotics is predicted to follow a square root[9,12,16,17]

$$S \propto \sqrt{\frac{T}{J}} \quad \text{for} \quad H = H_{c1} \quad \text{or} \quad H_{c2}. \tag{28}$$

Finally, in the gapped cases $0 \leq H < H_{c1}$ or $H > H_{c2}$, we expect activated behavior

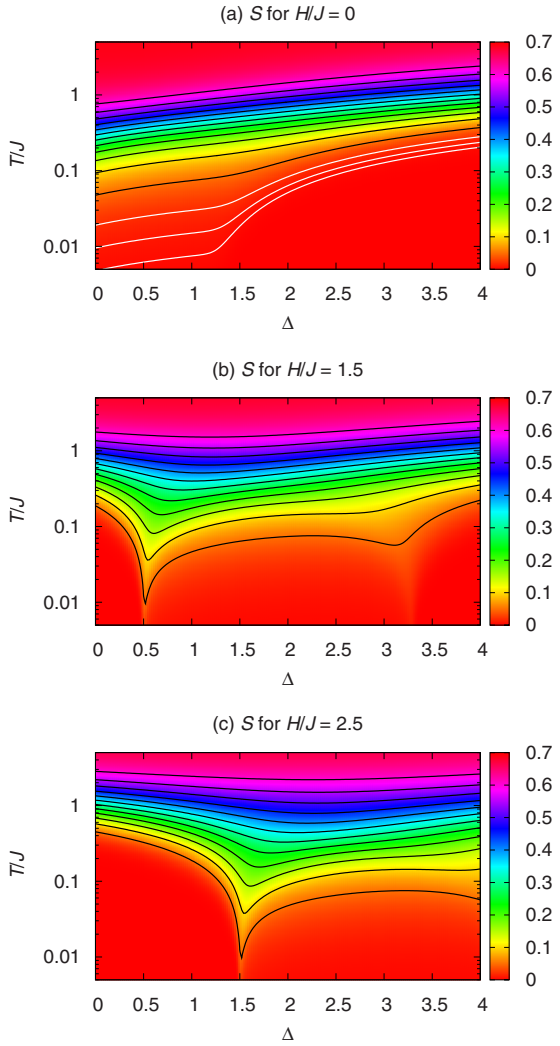

FIG. 6. (Color online) Entropy per spin $S(\Delta,T)$ for different values of (a) $H=0$, (b) $1.5J$, and (c) $2.5J$. The black lines are the isentropes for $S=0.05,0.1,\ldots,0.6$. Panel (a) contains three additional isentropes with $S=0.005$, 0.01, and 0.02 which are shown by white lines.

$$S \propto \exp(-G/T), \tag{29}$$

where G is the gap in the excitation spectrum. Closer inspection of the data shown in Figs. 5 and 6 indeed verifies Eq. (27), Eq. (28), or Eq. (29), respectively. Note that while the asymptotic behavior is $S\to 0$ for $T\to 0$ in all three cases, the decay is slowest exactly at the quantum phase transition, see Eq. (28). This naturally yields a maximum of the entropy S if the quantum phase transition is crossed by varying the parameters H or Δ at a fixed temperature $T>0$.

The case $\Delta=1$, $H=0$ is an exception to this general scenario. To first approximation, this point behaves like a Luttinger liquid. The fact that one is at a quantum critical point with marginally irrelevant operators gives rise to higher-order logarithmic corrections in the free energy and specific heat.[29,30] Consequently, one also expects just higher-order logarithmic corrections to the entropy. To test this scenario, we can use the fact that at $H=0$ the velocity v which enters

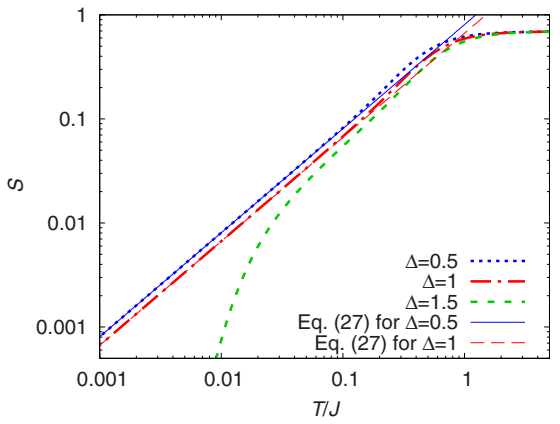

FIG. 7. (Color online) Entropy per spin S of the XXZ chain at $H=0$ for $\Delta=0.5$, 1, and 1.5. For $\Delta=0.5$ and 1 we also show the Luttinger-liquid expression (27) with the velocity v given by Eq. (30).

Eq. (27) is known exactly (see, e.g., Refs. 39 and 55),

$$v = \frac{\pi \sin\gamma}{2\gamma} J \tag{30}$$

with $\Delta=\cos\gamma$ as above. Figure 7 shows that insertion of these values of v into the Luttinger-liquid expression (27) yields indeed the correct low-temperature asymptotics of the entropy per spin at $H=0$ not only for $\Delta=0.5$ but also for $\Delta=1$. In fact, the higher-order logarithmic corrections to the Luttinger-liquid asymptotics [Eq. (27)] which are expected at $\Delta=1$ and $H=0$ are so small that they have no visible effect.

A gap G opens for $\Delta>1$ at $H=0$ but because the phase transition is a Kosterlitz-Thouless transition,[37,38] this gap is exponentially small close to $\Delta=1$.[35,36] Accordingly, close to $\Delta=1$ one has to go to very low temperatures in order to observe the crossover from Eq. (27) to Eq. (29). This is illustrated by the $\Delta=1.5$ curve in Fig. 7. In the concrete case $\Delta=1.5$, the value of the gap is $G\approx 0.087J$. Accordingly, the exponential decay [Eq. (29)] can be observed only for temperatures $T\lesssim 0.05J$ while at higher temperatures the behavior of $S(T)$ remains approximately linear.

The combined effect of all these observations is that just a small kink develops in the low-temperature isentropes of Fig. 6(a) whose position shifts very slowly to the quantum critical point $\Delta=1$ for $T\to 0$.

III. CONCLUSION AND PERSPECTIVES

Motivated by recent measurements of the magnetic cooling rate in a spin-$\frac{1}{2}$ Heisenberg chain compound,[15] we have presented an exact computation of the entropy and the magnetic cooling rate of the antiferromagnetic spin-$\frac{1}{2}$ XXZ chain in the thermodynamic limit $N\to\infty$. Furthermore, we have performed complementary numerical computations for the cooling rate of finite Heisenberg chains, namely, ED for small systems and QMC simulations for somewhat longer chains. We have demonstrated that we can obtain excellent approximations to the exact result with a combination of both numerical methods. On the one hand, this serves as a

consistency check of our computations. On the other hand, we are now in a position to apply a combination of ED and QMC to some minus-sign-free situations, such as the spin-$\frac{1}{2}$ Heisenberg model on the square and simple-cubic lattices where the exact methods are no longer applicable.

We have used the exact result for the entropy to illustrate that field-induced quantum phase transitions give rise to maxima of the low-temperature entropy or equivalently minima of the isentropes. This leads to cooling during adiabatic (de)magnetization processes where the lowest temperature is reached close to the quantum phase transition. As a consequence, we find a zero for the magnetic cooling rate at the phase transition and large positive (negative) values of the normalized cooling rate [Eq. (2)] for magnetic fields slightly above (below) the critical field.

The low-temperature asymptotics of the entropy S is exponentially activated in the gapped phases, linear in T in the gapless Luttinger-liquid regions, and follows the square-root behavior [Eq. (28)] at the field-induced quantum phase transitions. These asymptotic forms of $S(T)$ are expected to be universal for field-induced phase transitions in one-dimensional systems with U(1) symmetry[9,12,16,17] but can be particularly clearly verified with the aid of an exact solution.

The general features of the entropy should not depend on the specific choice of the magnetic field H as control parameter and indeed similar behavior is found as a function of the exchange anisotropy Δ. An exception is just the quantum phase transition at $H=0$ and $\Delta=1$ with Δ as a control parameter. Because this is a Kosterlitz-Thouless transition, only weak signatures are observed in the finite-temperature entropy.

Finally, closed-form expressions were derived in the Ising limit using the transfer-matrix method.[48,49] We have observed remarkably large magnetic cooling rates close to the field-induced critical point of the Ising chain. In fact, the transfer-matrix solution is closely related to a low-energy description of highly frustrated one-dimensional quantum antiferromagnets,[12,22,52–54] where enhanced cooling rates are observed as well.

ACKNOWLEDGMENTS

V.O. would like to thank the Institut für Theoretische Physik, Universität Göttingen and Universität Wuppertal for hospitality during the course of this work. This research stay was supported by the German Science Foundation (DFG). Furthermore, A.H. is grateful to the DFG (Grant No. HO 2325/4-1). V.O. was also supported by the CRDF under Grant No. UCEP-06/07 and ANSEF under Grant No. 1518-PS. C.T. would like to acknowledge support by the research program of the Graduiertenkolleg 1052 funded by the DFG.

[1] E. Warburg, Ann. Phys. Chem. **13**, 141 (1881).
[2] K. A. Gschneidner, Jr., V. K. Pecharsky, and A. O. Tsokol, Rep. Prog. Phys. **68**, 1479 (2005).
[3] A. M. Tishin and Y. I. Spichkin, *The Magnetocaloric Effect and its Applications* (Institute of Physics, Bristol, 2003).
[4] W. F. Giauque and D. P. MacDougall, Phys. Rev. **43**, 768 (1933).
[5] A. S. Oja and O. V. Lounasmaa, Rev. Mod. Phys. **69**, 1 (1997).
[6] T. Knuuttila, Ph.D. thesis, Helsinki University of Technology, 2000.
[7] P. Strehlow, H. Nuzha, and E. Bork, J. Low Temp. Phys. **147**, 81 (2007).
[8] A. M. Tishin, in *Handbook of Magnetic Materials*, edited by K. H. J. Buschow (Elsevier, Amsterdam, 1999), Vol. 12.
[9] J. C. Bonner and J. F. Nagle, Phys. Rev. A **5**, 2293 (1972).
[10] J. C. Bonner and M. E. Fisher, Proc. Phys. Soc. **80**, 508 (1962).
[11] J. C. Bonner and J. D. Johnson, Physica **86-88B**, 653 (1977).
[12] M. E. Zhitomirsky and A. Honecker, J. Stat. Mech.: Theor. Exp. (2004) P07012.
[13] A. S. Boyarchenkov, I. G. Bostrem, and A. S. Ovchinnikov, Phys. Rev. B **76**, 224410 (2007).
[14] A. Honecker and S. Wessel, Condens. Matter Phys. **12**, 399 (2009).
[15] Y. Tsui, B. Wolf, D. Jaiswal-Nagar, U. Tutsch, A. Honecker, K. Remović-Langer, G. Hofmann, A. Prokofiev, W. Assmus, G. Donath, and M. Lang (unpublished).
[16] L. Zhu, M. Garst, A. Rosch, and Q. Si, Phys. Rev. Lett. **91**, 066404 (2003).
[17] M. Garst and A. Rosch, Phys. Rev. B **72**, 205129 (2005).
[18] M. E. Zhitomirsky, Phys. Rev. B **67**, 104421 (2003).
[19] S. S. Sosin, L. A. Prozorova, A. I. Smirnov, A. I. Golov, I. B. Berkutov, O. A. Petrenko, G. Balakrishnan, and M. E. Zhitomirsky, Phys. Rev. B **71**, 094413 (2005).
[20] O. Derzhko and J. Richter, Eur. Phys. J. B **52**, 23 (2006).
[21] L. Čanová, J. Strečka, and M. Jaščur, J. Phys.: Condens. Matter **18**, 4967 (2006).
[22] O. Derzhko, J. Richter, A. Honecker, and H.-J. Schmidt, Low Temp. Phys. **33**, 745 (2007).
[23] M. S. S. Pereira, F. A. B. F. de Moura, and M. L. Lyra, Phys. Rev. B **79**, 054427 (2009).
[24] L. Čanová, J. Strečka, and T. Lučivjanský, Condens. Matter Phys. **12**, 353 (2009).
[25] A. Honecker and S. Wessel, Physica B **378-380**, 1098 (2006).
[26] B. Schmidt, P. Thalmeier, and N. Shannon, Phys. Rev. B **76**, 125113 (2007).
[27] M. Gaudin, Phys. Rev. Lett. **26**, 1301 (1971).
[28] M. Takahashi, *Thermodynamics of One-dimensional Solvable Models* (Cambridge University Press, Cambridge, 1999).
[29] A. Klümper, Eur. Phys. J. B **5**, 677 (1998).
[30] A. Klümper and D. C. Johnston, Phys. Rev. Lett. **84**, 4701 (2000).
[31] A. Klümper, Lect. Notes Phys. **645**, 349 (2004).
[32] J. D. Johnson and B. M. McCoy, Phys. Rev. A **6**, 1613 (1972).
[33] F. C. Alcaraz and A. L. Malvezzi, J. Phys. A **28**, 1521 (1995).
[34] D. C. Cabra, A. Honecker, and P. Pujol, Phys. Rev. B **58**, 6241 (1998).
[35] J. Des Cloizeaux and M. Gaudin, J. Math. Phys. **7**, 1384 (1966).
[36] C. N. Yang and C. P. Yang, Phys. Rev. **151**, 258 (1966).

[37] J. M. Kosterlitz and D. J. Thouless, J. Phys. C **6**, 1181 (1973).
[38] J. M. Kosterlitz, J. Phys. C **7**, 1046 (1974).
[39] F. D. M. Haldane, Phys. Rev. Lett. **45**, 1358 (1980).
[40] M. Troyer, B. Ammon, and E. Heeb, Lect. Notes Comput. Sci. **1505**, 191 (1998).
[41] A. F. Albuquerque, F. Alet, P. Corboz, P. Dayal, A. Feiguin, S. Fuchs, L. Gamper, E. Gull, S. Gürtler, A. Honecker, R. Igarashi, M. Körner, A. Kozhevnikov, A. Läuchli, S. R. Manmana, M. Matsumoto, I. P. McCulloch, F. Michel, R. M. Noack, G. Pawłowski, L. Pollet, T. Pruschke, U. Schollwöck, S. Todo, S. Trebst, M. Troyer, P. Werner, and S. Wessel, J. Magn. Magn. Mater. **310**, 1187 (2007).
[42] F. Alet, S. Wessel, and M. Troyer, Phys. Rev. E **71**, 036706 (2005).
[43] O. F. Syljuåsen and A. W. Sandvik, Phys. Rev. E **66**, 046701 (2002).
[44] P. Sengupta, A. W. Sandvik, and R. R. P. Singh, Phys. Rev. B **68**, 094423 (2003).
[45] M. Matsumoto and T. Nishimura, ACM Trans. Model. Comput. Simul. **8**, 3 (1998).
[46] S. Lukyanov, Nucl. Phys. B **522**, 533 (1998).
[47] J. Sirker and M. Bortz, J. Stat. Mech.: Theor. Exp. (2006) P01007.
[48] K. Huang, *Statistical Mechanics* (John Wiley & Sons, New York, 1963).
[49] R. Baxter, *Exactly Solved Models in Statistical Mechanics* (Academic, New York, 1982).
[50] J. Sznajd, Phys. Rev. B **78**, 214411 (2008).
[51] B. D. Metcalf and C. P. Yang, Phys. Rev. B **18**, 2304 (1978).
[52] O. Derzhko and J. Richter, Phys. Rev. B **70**, 104415 (2004).
[53] M. E. Zhitomirsky and H. Tsunetsugu, Phys. Rev. B **70**, 100403(R) (2004).
[54] M. E. Zhitomirsky and H. Tsunetsugu, Prog. Theor. Phys. Suppl. **160**, 361 (2005).
[55] T. Giamarchi, *Quantum Physics in One Dimension* (Clarendon, Oxford, 2004).